Mem. S.A.It. Vol. 76, 343

Memorie della

Accretion across the mass spectrum

A. Natta[1], L. Testi[1], S. Randich[1] and J. Muzerolle[2]

[1] INAF- Osservatorio di Arcetri, Largo Fermi 5, 50125 Firenze
[2] Steward Observatory, University of Arizona, 933 North Cherry Avenue, Tucson, AZ 85721, USA

Abstract. In this paper, we present first (and partial) results of a spectroscopic study in the near-IR and visual of a large sample (about 200 objects) of pre-main–sequence stars in Ophiucus. The accretion rate is determined using the luminosity of Paβ and the 10% width of Hα; both quantities are known to give reliable estimates of $\dot{M}_{ac}$ over a large range of masses. Our preliminary results seem to confirm that, for any given value of M_*, there is a large spread of possible values of $\dot{M}_{ac}$; however, the maximum observed $\dot{M}_{ac}$ decreases sharply with M_*.

Key words. Star Formation, Pre-main sequence stars, Accretion

1. Introduction

In recent years, there has been increasing evidence that the early phases of the evolution of objects of very low mass is not qualitatively different from that of their more massive counterparts, the T Tauri stars (TTS in the following). In this conference, several talks have shown observational evidence that sub-stellar objects have disks, accreting gas and, possibly, jets. All these phenomena characterize classical TTS, i.e., the evolutionary phase where accretion through a circumstellar disk is the main source of activity. This "T Tauri phase", as defined by Jayawardana et al. (2003), extends to the lowest mass objects studied so far.

Fig. 1 plots the accretion rate derived with a variety of techniques as function of the mass of the central objects for objects in Taurus, IC 348, Chamaeleon, Ophiucus (from Muzerolle et al. 2003; Natta et al. 2004); see also Muzerolle's poster in this conference). One can see that accretion rates can be measured in objects of few tens M_J(~0.03 $M_\odot$), extending the observed range well into the brown dwarf regime. These measurements show that there is no break in the strong correlation between the accretion rate and the mass of the central objects over a mass range of about two decades, and that young brown dwarfs accrete through their disk as scaled down versions of solar-mass stars. In addition, the accretion rates for brown dwarfs in Ophiucus seem larger than those for objects of similar mass in the older Taurus region; this, if confirmed, suggests that one can actually study how the accretion rate decreases with time over a large range of masses. These results give us crucial information that theoretical models of accretion disks need to address. However, the statistics are very poor both at the low-mass end of the spectrum, where very few objects in each star forming region have been analyzed, and for TTS in regions other than Taurus, where no

Send offprint requests to: A. Natta
Correspondence to: natta@arcetri.astro.it

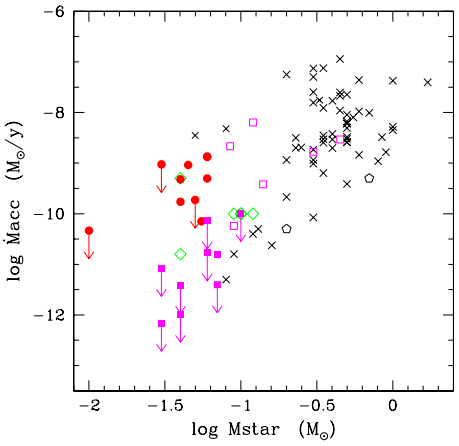

Fig. 1. Accretion rate as function of the mass of the central objects for Taurus (crosses), Ophiucus (dots), Chamaeleon I (filled and open squares), IC348 (diamonds), TWHya (pentagons). See Natta et al. (2004) and references therein.

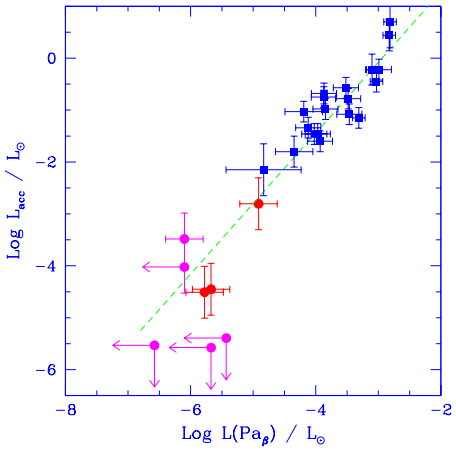

Fig. 2. Accretion luminosity as function of the Paβ luminosity. Squares are TTS in Taurus from Muzerolle et al. (1998); dots are objects in Ophiucus and ChaI from Natta et al. (2004). The dashed line is the best-fit relation.

quantitative estimates of the accretion rate are available.

2. An IR Pilot Project

Ophiucus is one of the youngest, nearby star forming regions. Its core contains several hundred objects (Luhman and Rieke 1999); it has been imaged in the mid-infrared with ISOCAM by Bontemps et al. (2001), who detected 425 sources. Some of these sources have masses in the brown dwarf range (Comerón et al. 2000; Natta et al. 2003). Ophiucus is perfectly suited for a study of the accretion properties of a large sample of very young objects covering a broad range of masses. There is, however, a serious limitation, because the region has very high extinction, and the classical methods of measuring the accretion rate from veiling or the Hα profile (e.g., Gullbring et al. 1998; Muzerolle et al. 2001) are only applicable to a limited subset of objects.

We have therefore started a program aimed at measuring accretion rates using hydrogen infrared lines, such as Paβ at 1.28 μm and Brγ at 2.17 μm. Muzerolle et al. (1998) have shown that the luminosity of these lines is a good tracer of the accretion luminosity for TTS in Taurus. In our pilot program, we obtained the Paβ luminosity of a small sample of spectroscopically characterized brown dwarfs in Ophiucus and Chamaeleon, for which we also obtained high resolution Hα profiles. The accretion rates derived by fitting Hα profiles with magnetospheric models were converted to accretion luminosity, using the appropriate stellar parameters, and plotted as function of the observed Paβ luminosity. The results (Fig. 2) showed that the Muzerolle et al. (1998) correlation extends to the lowest observable masses, and that the luminosity of the hydrogen infrared lines can be used to determine accretion luminosities and mass accretion rates for a large sample of embedded pre-main sequence stars of all masses.

3. The Large Ophiucus Sample

Encouraged by the results of the pilot project, we have selected about 200 objects in Ophiucus from the ISOCAM sample of

Bontemps et al. (2001), for which we obtained near-IR spectra (mostly Paβ, in some cases Brγ) with ISAAC at VLT and SOFI at NTT (R$\sim$1000) and optical high resolution spectra of Hα using FLAMES+Giraffe and UVES on VLT (R$\sim$ 30000-40000). The distribution of the sample among Class I, II and III is shown in Fig. 3 as function of the luminosity of the objects, as estimated by Bontemps et al. (2001). The classification of any given object is based on its mid-infrared colors; Class I objects have colors typical of embedded protostars, Class II of classical TTS and Class III of stellar photospheres.

Fig. 4 shows the distribution in mass of the Class II and Class III sources in our sample. We have estimated the mass of each object by placing it on the HR diagram on a 0.5 Myr isocrone (Luhman and Rieke 1999; Bontemps et al. 2001) and deriving the effective temperature and mass which correspond to the Bontemps et al. (2001) luminosity. This is a very crude procedure, which will be improved once the spectral classification of all the objects is completed. However, it is useful for a first characterization of our sample. The median mass is roughly 0.2 $M_\odot$, and all masses below about 0.8 $M_\odot$ are well represented. However, one should keep in mind that the Bontemps et al. (2001) sample is not complete at the lower mass end. This incompletness is particularly severe for Class III objects, which lack, by definition, a mid-IR excess and can only be detected by ISOCAM if luminous (i.e., massive) enough.

Only part of the data has been reduced so far, and any conclusion is premature. There are, however, a couple of points worth mentioning. First of all, only one Class III object of the 35 analyzed so far has Paβ in emission. The hydrogen infrared lines are seen in emission only in Class II objects, i.e., when there is evidence from the mid-IR colors of the presence of a circumstellar disk. However, about 40% of Class II are not detected. It seems, therefore, that Paβ (or Brγ) emission is only shown by accreting objects, but a census of accreting objects based on Paβ will miss about 40% of them. It should be pointed out that our observations can only detect lines with equivalent width $\gtrsim$0.3–0.5 Å,

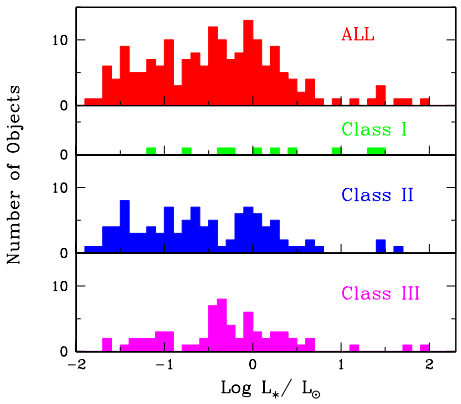

Fig. 3. Luminosity distribution of the Ophiucus sample.

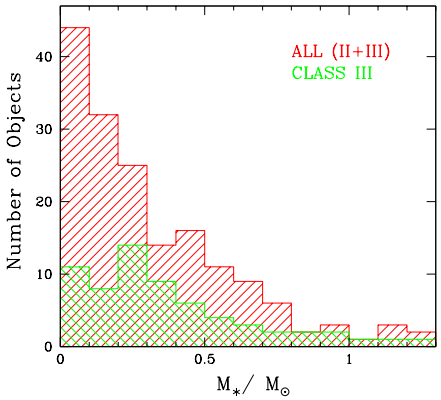

Fig. 4. Distribution in mass of the observed sample (Class II + Class III: hatched; Class III only: cross-hatched).

and that we need to understand how systematic effects (such as veiling due to disk emission), affect our statistics.

For the objects analyzed so far, we have computed the accretion rate from the Paβ luminosity as discussed in Natta et al. (2004). Fig. 5 shows the results as function of the mass

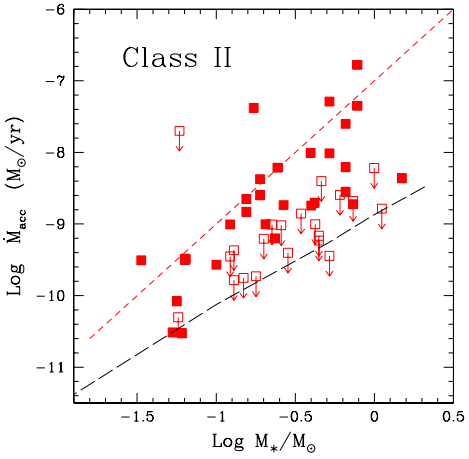

Fig. 5. Mass accretion rate for Class II objects derived from Paβ luminosity as in Natta et al. (2004). Open squares are 3σ upper limits. The short-dashed line shows the slope of a $\dot{M}_{ac} \propto M_*^2$ relation. The long-dashed line is an estimate of the $\dot{M}_{ac}$ detection limit corresponding to a Paβ equivalent width of 0.5 Å.

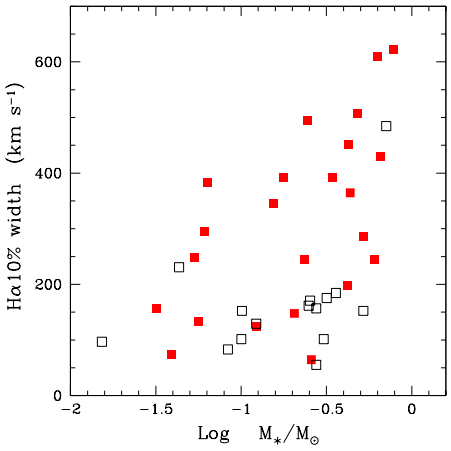

Fig. 6. 10% full width as function of the mass of the central object for Class II (filled squares) and Class III (open squares) sources.

of the central object. The trend of increasing $\dot{M}_{ac}$ for increasing M_* is clearly confirmed. However, there is a large spread of $\dot{M}_{ac}$ for objects of similar mass, which is clearly seen for large values of M_*, where our detection limit (long-dashed line) is significantly lower than the largest observed values. For example, for $M_* \sim 0.5\ M_\odot$, $\dot{M}_{ac}$ varies by more than 2 orders of magnitude. A similar spread was also found in TTS in Taurus (see, e.g., White and Ghez 2001 and Muzerolle et al. 2001).

For about 140 objects, 70% of which have also been observed in the near-IR, we have obtained Hα profiles. Also these data have been reduced only in part. Fig. 6 plots the 10% full width of Hα as function of M_*. Hα is rather narrow (10% full width < 200 km s^{-1}) in Class III objects of all mass (with one exception); it is generally broader in Class II objects, with a trend of broader lines in more massive objects. The Hα 10% width can also be used to estimate $\dot{M}_{ac}$ (Natta et al. 2004). Fig. 7 plots Hα-derived $\dot{M}_{ac}$ as function of M_* for Class II objects with 10% width>250 km s^{-1}, which is generally considered the limit separating Hα emission due to chromospheric activity from magnetospheric accretion (see White and Basri 2003). The correlation of $\dot{M}_{ac}$ with M_* is clearly present, as well as the large spread of $\dot{M}_{ac}$ seen in Fig. 5.

4. Final Considerations

We should stress that the results presented here for our large Ophiucus sample are very preliminary. In particular, the determination of masses using "statistical" methods is only valid to zero order, and one needs to obtain the spectral type of individual objects to compute more reliable masses, before any firm conclusion could be reached.

At this stage, our observations of pre-MS objects in Ophiucus seem to confirm that Class II objects of all masses are accreting, with maximum accretion rate decreasing sharply for objects of lower mass. For any value of M_* there is a large spread of $\dot{M}_{ac}$, and the relation $\dot{M}_{ac} \propto M_*^2$ likely characterizes the upper envelope of the distribution only. Still, its implication for the mechanisms regulating angular momentum dissipation in disks and the nature of accretion need to be understood. Viscous

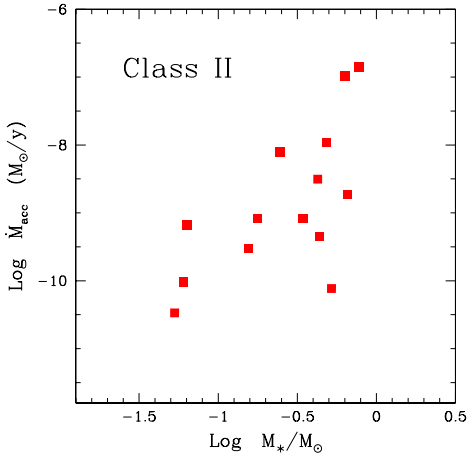

Fig. 7. Accretion rate for Class II sources derived from the Hα 10% width following Natta et al. (2004). Only objects with 10% width >250 km s^{-1} have been included.

disk models with constant viscosity parameter α predict a rather shallow dependence of $\dot{M}_{ac}$ on M_*(roughly as $M_*^{0.9}$ for reprocessing disks). Muzerolle et al. (2003) suggest that different levels of ionization due to the X-ray emission of the central object could cause a steeper dependence of $\dot{M}_{ac}$ on M_*. Very recently, Padoan et al. (2004) propose that accretion in classical TTS disks is controlled by Bondi-Hoyle accretion from the large scale gas distribution in the parent cloud. All these are interesting possibilities, that need to be explored further.

Acknowledgements. This work was partly supported by the MIUR-cofin grant "Low-mass stars and brown dwarfs: formation mechanisms, mass distributio n and activity".

References

Bontemps, S., André, Ph., Kaas, A.A., et al. 2001, A&A 372, 173
Comerón, F., Neuhäuser, R., & Kaas, A.A. 2000, A&A, 359, 269
Gullbring, E., Hartmann, L., Briceño, C., & Calvet, N. 1998, ApJ 492, 323
Jayawardhana, R., Mohanty, S., & Basri, G. 2003, ApJ 592, 282
Luhman, K.L., & Rieke, G.H. 1999, ApJ 525, 440
Muzerolle, J., Hartmann, L., & Calvet, N. 1998, AJ 116, 455
Muzerolle, J., Calvet, N., & Hartmann, L. 2001, ApJ 550, 944
Muzerolle, J., Hillenbrand, L., Calvet, N., Briceo, C., & Hartmann, L. 2003, ApJ 592, 266
Natta, A., Testi, L., Comerón, et al. 2003, A&A 393, 597
Natta, A., Testi, L., Muzerolle, J., Randich, S., Comerón, F., & Persi, P. 2004, A&A
Padoan, P., Kritsuk, A., Norman, M.L. & Nordlund, A. 2004, ApJL, submitted
White, R.J., & Basri, G. 2003, ApJ 582, 1109
White, R.J., & Ghez, A. 2001, ApJ 556, 265